



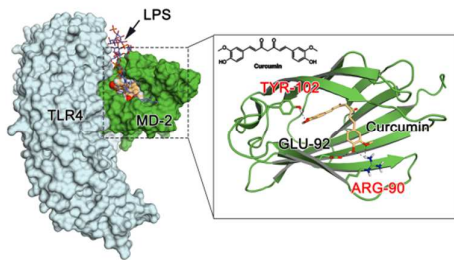
**Insights into the binding mode of curcumin to MD-2: studies
from molecular docking, molecular dynamics simulations
and experimental assessments**

Journal:	<i>Molecular BioSystems</i>
Manuscript ID:	MB-ART-01-2015-000085.R2
Article Type:	Paper
Date Submitted by the Author:	14-Apr-2015
Complete List of Authors:	<p>Wang, Zhe; Wenzhou Medical University, School of Pharmaceutical Sciences Chen, Gaozhi; Wenzhou Medical University, School of Pharmaceutical Sciences Chen, Linfeng; Wenzhou Medical University, School of Pharmaceutical Sciences Liu, Xing; Wenzhou Medical University, School of Pharmaceutical Sciences Fu, Weitao; Wenzhou Medical University, School of Pharmaceutical Sciences Zhang, Yali; Wenzhou Medical University, School of Pharmaceutical Sciences Li, Chenglong; Ohio State University, College of Pharmacy Liang, Guang; Wenzhou Medical University, School of Pharmaceutical Sciences Cai, Yuepiao; Wenzhou Medical University, School of Pharmaceutical Sciences</p>

Insights into the binding mode of curcumin to MD-2: studies from molecular docking, molecular dynamics simulations and experimental assessments

Zhe Wang,^{a,#} Gaozhi Chen,^{a,#} Linfeng Chen,^a Xing Liu,^a Weitao Fu,^a Yali Zhang,^a Chenglong Li,^{b,a} Guang Liang,^{a*} and Yuepiao Cai^{a*}

The residues R90 and Y102 of MD-2 are hot spot residues that contribute significantly to the affinity of curcumin's binding.





Journal Name

ARTICLE

Insights into the binding mode of curcumin to MD-2: studies from molecular docking, molecular dynamics simulations and experimental assessments

Received 00th January 20xx,
Accepted 00th January 20xx

DOI: 10.1039/x0xx00000x

www.rsc.org/Zhe Wang,^{a,#} Gaozhi Chen,^{a,#} Linfeng Chen,^a Xing Liu,^a Weitao Fu,^a Yali Zhang,^a Chenglong Li,^{b,a} Guang Liang,^{a*} and Yuepiao Cai^{a*}

Curcumin, a natural product, has been shown to possess notable anti-inflammatory activities and numerous studies have been carried out on its clinical applications. Recently, several reports mentioned that myeloid differentiation protein 2 (MD-2) may be the direct target of curcumin in the inhibition of lipopolysaccharide (LPS) signaling. However, the exact interaction between curcumin and MD-2 is still incompletely understood. In present study, computational and experimental methods were employed to explore the underlying structural mechanism of curcumin binding to MD-2 protein. Molecular docking and molecular dynamics (MD) simulations studies showed that curcumin could be embed into the hydrophobic pocket of MD-2 and form stable hydrogen bonding interactions with the residues R90 and Y102 of MD-2. Moreover, experimental results of curcumin binding to MD-2^{R90A/Y102A} mutant further confirmed that the residues ARG-90 and TYR-102 contribute to the recognition process of curcumin binding to MD-2 protein. In conclusion, we have explored the binding mechanism of curcumin binding to MD-2; more importantly, this work could offer useful references for designing novel analogs of curcumin as potential anti-inflammatory agents targeting MD-2 protein.

Introduction

Toll-like receptors (TLRs) as one of the pattern recognition receptors play critical roles in the recognition of conserved pathogen-associated molecular patterns derived from diverse microbial pathogens and in the ensuing initiation of innate immune responses.¹ Among TLRs, Toll like receptor 4 (TLR4) is the most extensively investigated receptor and also the central signaling receptor for the gram-negative bacterial lipopolysaccharide (LPS) which can induce sepsis.^{2,3} However, it is proved that TLR4 alone is not sufficient for the recognition of LPS and the co-receptor myeloid differentiation protein 2 (MD-2) is absolutely required to sense the lipid A domain of LPS.^{4,5} MD-2, a small protein, contains 143 amino acid residues that adopt a β cup fold with two antiparallel β sheets and constructs a hydrophobic pocket.^{6,7} The engagement of LPS with TLR4/MD-2 complexes leads to the dimerization of two TLR4/MD-2 complexes and the activated receptor multimer recruits two major adaptor molecules, MyD88 and TRIF.⁸ The intracellular signaling pathways activate the transcription factors such as nuclear factor- κ B (NF- κ B) and IFN regulatory factor 3 (IRF3), which regulate the expression of inflammatory cytokines and eventually lead to the

progression of inflammatory diseases.^{9,10}

Curcumin (**Fig. 1A**) is an extended pseudo symmetric polyphenol derived from the turmeric rhizome of the herb *Curcuma Longa*.¹¹ Its multiple pharmacological activities and medicinal applications have attracted attentions of various researchers.¹²⁻¹⁴ Over the last decades, it has been reported that curcumin has therapeutic effects in various diseases such as diabetes, liver diseases, rheumatoid diseases, atherosclerosis, infectious diseases and cancers.^{15,16} As a highly pleiotropic molecule, curcumin affects a wide range of molecular targets, including transcriptional factors, inflammatory cytokines, receptors, enzymes, growth factors and kinases.¹⁷ However, as far as we know, it is still very difficult to clarify its exact targeting and binding mechanisms. Due to the lack of structural information of curcumin and its receptor complex, it's almost impossible to carry out structure-based rational drug design analyses, which largely slows down the development efficiency of curcumin derivatives into clinic applications.

More recently, Gradisar and his colleagues have demonstrated that curcumin binds directly to MD-2 through a noncovalent mechanism and antagonizes the cellular responses to LPS depending upon both MyD88 and TRIF.¹⁸ From this point of view, MD-2 is proposed as a potential target for a therapy that neutralizes toxic effects of the endotoxin. It is reported that curcumin, like other three nolipid compounds (JSH, xanthohumol, and isoxanthohumol), linearly aligns at the mouth to the bottom inside the MD-2 pocket.¹⁹ However, the exact atomic interactions between curcumin and MD-2 are still unclear. In the present study, computational and experimental

^aChemical Biology Research Center, School of Pharmaceutical Sciences, Wenzhou Medical University, Wenzhou, Zhejiang 325035, China
E-Mail: ypcal@wmu.edu.cn, wzmcclianguang@163.com

^bDivision of Medicinal Chemistry and Pharmacognosy, College of Pharmacy, Ohio State University, Columbus, Ohio 43210, United States

methods were employed to explore the underlying structural mechanisms of curcumin binding to the MD-2 protein. Molecular docking and molecular dynamics simulations were used to predict the possible binding features. On the other hand, experimental assessments were carried out to affirm our theoretical hypothesis. It is expected that this work can provide some valuable guidance on the design of more promising MD-2 inhibitors as potential anti-inflammatory agents.

Insert Fig. 1

Fig. 1 Curcumin shows a MD-2 inhibition activity by binding to the MD-2. (A) The structure of curcumin. (B) The surface plasmon resonance (SPR) analysis shows the direct interaction between curcumin and MD-2 WT protein. (C) The ELISA assay shows that curcumin inhibits the Biotin-LPS binding to MD-2^{WT}. Data are mean values (\pm SEM) of at least 3 separate repeating experiments (** $P < 0.01$).

Materials and methods

Reagents

The mouse RAW 264.7 macrophages were purchased from ATCC (Manassas, VA). Recombinant human MD-2 (rhMD-2, or rhMD-2 mutant) proteins were purchased from Biowit Technologies (Shenzhen, China). Curcumin, LPS (from *Salmonella typhosa*). The Anti-MD-2 antibody was purchased from eBioscience (San Diego, CA).

Surface plasmon resonance analysis (SPR)

The binding affinity of curcumin to rhMD-2 and rhMD-2 mutants were determined via a ProteOn XPR36 Protein Interaction Assay system (Bio-Rad Laboratories, Hercules, CA) with a HTE sensor chip (ProteOn™, #176-5033). Briefly, the rhMD-2 protein (in acetate acid buffer pH 5.5) was loaded onto the sensors which were activated by 10 mM NiSO₄. The curcumin samples (at 100, 75, 50, 25, 12.5, and 0.0 μ M) were prepared with a running buffer (PBS, 0.005% SDS, 5% DMSO). The sample plates were placed on the instrument. The interactions were determined according to the instructions of the manufacturer, at a flow rate of 30 μ L/min for 120 s during the association phase followed by 120 s for the dissociation phase at 25 °C. The data were analysed with the ProteOn manager software. Binding kinetic parameters the equilibrium constant K_D values were calculated by a global fitting of the kinetic data from various concentrations of curcumin using a 1:1 Langmuir binding model.

Enzyme-linked immunosorbent assay (ELISA)

In a cell-free assay of LPS binding to MD-2, the anti-human MD-2 antibody (eBioscience, San Diego, CA) was coated in a 96-well plate overnight at 4 °C in a 10 mM Tris-HCl buffer (pH 7.5). The plate was washed with PBST and blocked with 3 % BSA for 1.5 h at room temperature. rhMD-2 (4 μ g/mL) in 10 mM Tris-HCl buffer (pH 7.5) was added to the pre-coated plate

and incubated for 1.5 h at room temperature. After being washed with PBST, biotin-labeled LPS (Biotin-LPS, InvivoGen, San Diego, CA) was incubated for 1 h at room temperature with or without the presence of curcumin (0.1 or 1.0 μ M). After further washing, streptavidin-conjugated horseradish peroxidase (Beyotime, Shanghai, China) was added for 1 h at room temperature. The horseradish peroxidase activity was determined in a M5 microplate reader at 450 nm after the addition of TMB substrate solution (eBioscience, San Diego, CA).

Molecular docking

The molecular docking simulation was carried out by using AutoDock version 4.2.6.²⁰ The crystal structure of human MD2-lipid IVa complex (PDB code 2E59) was derived from Protein Data Bank as the receptor in the current docking model. AutoDockTools version 1.5.6²⁰ was employed to generate the docking input files and to analyze the docking results. A grid box size of 60 \times 60 \times 60 points with a spacing of 0.375 Å between the grid points was implemented and covered almost the entire protein-binding site. The affinity maps of MD-2 were calculated using AutoGrid. Lamarckian Genetic Algorithm (LGA) adds a local minimization to the genetic algorithm, enabling the modification of the gene population. The docking parameters were as follows: trials of 100 dockings, the population size of 150, the random starting position and conformation, mutation rate of 0.02, the crossover rate of 0.8, the local search rate of 0.06, and 25 million energy evaluations. Final docked conformations were clustered using a tolerance of 1.5 Å root-mean-square deviations (RMSD). A reasonable pose was selected for the detailed analysis and further studies.

Molecular dynamics simulations

The docked structures of the curcumin/MD-2 complexes and the apo MD-2 protein were used as the starting conformations for MD simulations. The electrostatic potentials (ESP) of curcumin were calculated at the Hartree-Fock level with the 6-31G* basis set using NWChem 6.1.1.²¹ The general AMBER force field (gaff)²² and the ff99SB force field²³ were used for the ligand and protein, respectively. The parameters of curcumin were assigned by the restrained Electrostatic potential (RESP) procedure with partial charges fitted using the ANTECHAMBER module in the AMBER 11.²⁴ All the missing hydrogen atoms were added using the LEaP program in AMBER 11.²⁴ The complex was solvated in a box of TIP3P water molecules with a hydration shell of 10 Å and then was neutralized by adding an appropriate number of chloride ions.²⁵

All the energy minimizations and MD simulations were performed with the AMBER 11 packages²⁴ using the GPU accelerated codes of the PMEMD program.²⁶ The whole systems were minimized in two stages to remove bad contacts. At first, the water molecules were minimized by restraining the protein with a restraint constant of 2.0 kcal \cdot mol⁻¹ \cdot Å⁻² by using the steepest descent minimization of 1000 steps followed by a conjugate gradient minimization of 1000 steps; secondly, the entire systems were minimized without any restriction by 2000

steps starting with the steepest descent minimization followed by the conjugate gradient minimization after 2000 cycles. The systems were then heated gradually from 0 to 300 K in the NVT ensemble in 100 ps and equilibrated at 300 K for 200 ps in the NPT ensemble, and then 50 ns MD simulations were performed at a constant temperature of 300 K and a constant pressure of 1 atm. Particle mesh Ewald (PME) was employed to deal with the long-range electrostatic interactions under periodic boundary conditions.²⁷ The SHAKE method was used to constrain hydrogen atoms and the time step was set to 2 fs.²⁸ The coordinates were saved every 10 ps for the subsequent analysis.

Results and discussion

The direct binding of curcumin to MD-2

Recently, Helena Gradišar and her co-workers have reported that MD-2 is the target of curcumin in the inhibition of the response to LPS.¹⁸ Here, we carried out several biochemical experiments at the molecular level to test the direct interactions between curcumin and MD-2. We evaluated the binding affinity of curcumin with MD-2 by SPR experiments, which exhibited that curcumin binds MD-2 protein in a dose-dependent manner with a relatively high affinity and the K_D value of 0.000379M (Fig. 1B). This result validated that there is a direct binding of curcumin to the recombinant MD-2 protein. In addition, we established a biotin-streptavidin-based ELISA system for the determination of LPS-rhMD-2 interaction. Fig. 1C showed that Biotin-marked LPS (Biotin-LPS) bound to rhMD-2 in the plates, while its co-incubation with curcumin significantly blocked the interactions of Biotin-LPS and rhMD-2. This also suggests the binding site for curcumin on MD-2 may overlap with the binding site for LPS.

The binding mode of curcumin to MD-2

The molecular docking is a popular and effective method to predict for predicting the binding mode of the ligand to its receptor.^{29,30} In order to explore the binding mode of curcumin and MD-2, the molecular docking was performed and the docking results were shown in Fig. 2. Curcumin can be inserted into the large hydrophobic binding pocket of MD-2 by occupying a large part of the binding site of LPS (Fig. 2A). Moreover, curcumin can form multiple hydrogen bonds with residues ARG-90, GLU-92 and TYR-102 of MD-2 (Fig. 2B). Interestingly, Michael R. Peluso et al. reported that xanthohumol and related prenylated flavonoids have the same interactions with the residue TYR-102 of MD-2.³¹ This indicates to us that TYR-102 may be a crucial residue for ligands binding with MD-2. In line with our expectation, the potential binding mode between curcumin and MD-2 was obtained by the docking study. Then, we selected the docked complex with the lowest binding energy to conduct the following MD simulations.

Insert Fig. 2

Fig. 2 The docking mode of curcumin to the activity cavity of MD-2. (A) Curcumin overlapped with LPS in binding site of MD-2 together with TLR4. TLR4 and MD-2 are shown with the cyan and green surface. LPS is shown with blue sticks and curcumin is shown with yellow spheres, respectively. (B) The detailed interactions between curcumin and MD-2. MD-2 is shown with green cartoon and curcumin is represented with yellow sticks. Hydrogen bonds are depicted with black dotted lines.

The stability of the docked complex

The stability of the docked complex can be evaluated by MD simulations since an improperly docked conformation is expected to produce an unstable trajectory.^{32,33} Based on this consideration, conventional MD simulations of two systems, curcumin-MD-2 and apo MD-2, were carried out in the explicit water for 50 ns. The root-mean square deviation (RMSD) for all $C\alpha$ atoms of protein and all heavy atoms of curcumin in relation to the initial structure against simulation time were detected. As shown in Fig. 3A, the $C\alpha$ atom RMSD values for the curcumin and MD-2 gradually became stable after 30 ns, with the RMSD values of 2.5 Å and 0.4 Å, respectively. However, the corresponding RMSD values of protein in the apo MD-2 system tended to converge at 4.0 Å after 30 ns simulations (see in Fig. 3B).

Insert Fig. 3

Fig. 3 The time dependence of RMSDs for $C\alpha$ atoms of protein and heavy atoms of ligand. (A) Time evolution of the RMSD of MD-2 and curcumin are shown with black lines and red lines, respectively. (B) The time evolution of the RMSD of apo MD-2. The alignments of starting (green cartoon) and final (margin cartoon) structures. (C) The Curcumin-MD-2 complex system. (D) The Apo MD-2 system.

In order to get a deeper insight into the structural fluctuations we conducted the structure alignments for the first and the last snapshots of MD simulations (Fig. 3C and 3D). As shown in the figure, the apo MD-2 makes a great conformational change while the structure of curcumin-MD2 complex is very stable. It can be obviously noted that the docked complex and the last snapshot of MD simulation structure were well overlapped at the same binding site of MD-2 with only slight positional derivations, which further verified the reasonableness and the stability of the docking results. On the other hand, the final structure of the apo MD-2 exhibits a significant narrowing of the cavity entrance and destabilization of the β -hairpins at the mouth, which was consistent with the research results of Teresa Paramo and his colleagues.³⁴ This suggests that curcumin can not only bind to MD-2, but also play an important role in stabilizing the open conformation of MD-2.

Hydrogen bonds are important indicators of nonbonding interactions between the proteins and ligands, and play critical roles in the protein–ligand recognition process.³⁵ To further

explore the hydrogen bonding interactions between curcumin and MD-2, the hydrogen bond analysis was carried out. The distances of atoms, which can form hydrogen bonds in docking complex, were monitored during the whole process of the MD simulations and plotted in Fig. 4. As shown in Fig. 4A, the hydrogen bonding interactions between oxygen atoms in hydroxyl and methoxy groups (O3 and O5) of curcumin and residues ARG-90 and TYR-102 of MD-2 were extremely stable along the 50 ns MD simulations with a distance of about 3 Å. The detailed distance evolutions of the two hydrogen bonds were illustrated in Fig. 4B and 4C, respectively. In addition, the average distances between heavy atoms and the occupancies for the hydrogen bonding interactions in the simulated system were calculated (see in Table 1). However, it is remarkable that the hydrogen bond between curcumin and residue GLU-92 in docking complex was not strong enough to be maintained and broken quickly at the beginning of MD simulations.

Insert Fig. 4

Fig. 4 Analysis of key hydrogen bonding interactions between curcumin and MD-2. (A) curcumin is shown with green sticks, and residues ARG-90 and TYR-102 are shown with white sticks covered with transparent surface. Hydrogen atoms are omitted and hydrogen bonds are depicted by black dotted lines. (B) The distance changes for the hydrogen bonds between curcumin and residue ARG-90. (C) The distances for the hydrogen bonds between curcumin and residue TYR-102.

Table 1 Summary of the average distances between heavy atoms (Å) and percent of occurrence data (%) for the hydrogen bonding interactions in the simulated system^a

Insert Table 1

^a Hydrogen bond criteria are 3.5 Å for donor-acceptor distance and 120° for donor-H-acceptor angle.

The weak interaction between curcumin and MD-2^{R90A/Y102A} mutant

Taking into account the computational results, we suggested that residues ARG-90 and TYR-102 play a pivotal role in curcumin binding to MD-2. In order to confirm our hypothesis, a MD-2 double mutant protein MD-2^{R90A/Y102A} was prepared for the further binding affinity determination between curcumin and MD-2 mutant. As shown in Fig. 5A, SPR analysis indicated that the high affinity between curcumin and MD-2 was definitely declined (more than 5,000 times) when curcumin was binding to the MD-2^{R90A/Y102A} mutant. Further ELISA assay exhibited that curcumin could not block the binding of biotin-LPS with the MD-2^{R90A/Y102A} mutant (Fig. 5B). In the mutant system, the key hydrogen bond interactions between curcumin and MD-2 no longer exist which led to a huge decrease in the binding affinity. These results demonstrated that the residues ARG-90 and TYR-102 exactly contribute to the recognition process of curcumin binding to MD-2 protein.

Insert Fig. 5

Fig. 5 Curcumin exhibits a low binding affinity to MD-2^{R90A/Y102A} mutant. (A) The surface plasmon resonance (SPR) assay showed that the R90A and Y102A mutant of MD-2 lost the high affinity between curcumin and MD-2 protein. (B) The ELISA assay showed that curcumin scarcely inhibited the Biotin-LPS binding to MD-2^{R90A/Y102A} mutant. The data are mean values (±SEM) of at least 3 separate repeated experiments.

Conclusions

In this study, we combine computational and experimental methods to identify the important binding site residues and the binding mode of the curcumin to MD-2. We performed molecular docking to predict a possible binding mode of curcumin-MD-2 complexes. In addition, molecular dynamics simulations were used to indicate the complexes obtained from the docking study were stable. Our simulation results indicated that two steady hydrogen binding interactions were critical to maintain the binding mode of ligand and protein. Furthermore, the SPR assay and ELISA assay using recombinant MD-2 site-directed mutants demonstrated that Arg-90 and Tyr-102 in MD-2 protein are indeed key residues which contribute to stabilize the curcumin-MD-2 complexes via forming two main hydrogen bonds. The results obtained from this study will be valuable for the future rational design of novel and potent MD-2 inhibitors as promising anti-inflammatory therapeutics.

Acknowledgements

This study was supported, in part, by the National Natural Science Funding of China (81473242 to Y.C., 81173083 to Y.C., and 21272179 to G.L.), High-level Innovative Talent Funding of Zhejiang Department of Health (2010-190-17 to G.L.), Zhejiang Natural Science Funding (LY14C050004 to X.L. and LQ14H310003 to Y.Z.), and Zhejiang College Students' Science and Technology Innovation Activities Program (2014R413047 to Z.W.).

Notes and references

1. S. Akira and K. Takeda, *Nature Reviews Immunology*, 2004, 4, 499-511.
2. Y. Tan and J. C. Kagan, *Molecular cell*, 2014, 54, 212-223.
3. B. S. Park and J. O. Lee, *Experimental & molecular medicine*, 2013, 45, e66.
4. G. Duan, J. Zhu, J. Xu and Y. Liu, *Frontiers in bioscience*, 2014, 19, 904-915.
5. B. S. Park, D. H. Song, H. M. Kim, B. S. Choi, H. Lee and J. O. Lee, *Nature*, 2009, 458, 1191-1195.
6. U. Ohto, K. Fukase, K. Miyake and Y. Satow, *Science*, 2007, 316, 1632-1634.
7. H. M. Kim, B. S. Park, J. I. Kim, S. E. Kim, J. Lee, S. C. Oh, P. Enkhbayar, N. Matsushima, H. Lee, O. J. Yoo and J. O. Lee, *Cell*, 2007, 130, 906-917.
8. E. F. Kenny and L. A. O'Neill, *Cytokine*, 2008, 43, 342-349.

9. F. Peri and V. Calabrese, *Journal of medicinal chemistry*, 2014, 57, 3612-3622.
10. S. H. Park, M. S. Kyeong, Y. Hwang, S. Y. Ryu, S. B. Han and Y. Kim, *Biochemical and biophysical research communications*, 2012, 419, 735-740.
11. A. H. Rahmani, M. A. Al Zohairy, S. M. Aly and M. A. Khan, *BioMed research international*, 2014, 2014, 761608.
12. K. G. Troselj and R. N. Kujundzic, *Current pharmaceutical design*, 2014, 20, 6682-6696.
13. L. N. Sun, Z. Y. Yang, S. S. Lv, X. C. Liu, G. J. Guan and G. Liu, *International immunopharmacology*, 2014, 23, 236-246.
14. D. Akbik, M. Ghadiri, W. Chrzanowski and R. Rohanizadeh, *Life sciences*, 2014, DOI: 10.1016/j.lfs.2014.08.016.
15. A. Noorafshan and S. Ashkani-Esfahani, *Current pharmaceutical design*, 2013, 19, 2032-2046.
16. H. P. Ammon and M. A. Wahl, *Planta medica*, 1991, 57, 1-7.
17. B. B. Aggarwal and B. Sung, *Trends in pharmacological sciences*, 2009, 30, 85-94.
18. H. Gradisar, M. M. Keber, P. Pristovsek and R. Jerala, *Journal of leukocyte biology*, 2007, 82, 968-974.
19. S. H. Park, N. D. Kim, J. K. Jung, C. K. Lee, S. B. Han and Y. Kim, *Pharmacology & therapeutics*, 2012, 133, 291-298.
20. G. M. Morris, R. Huey, W. Lindstrom, M. F. Sanner, R. K. Belew, D. S. Goodsell and A. J. Olson, *Journal of computational chemistry*, 2009, 30, 2785-2791.
21. M. Valiev, E. J. Bylaska, N. Govind, K. Kowalski, T. P. Straatsma, H. J. Van Dam, D. Wang, J. Nieplocha, E. Apra and T. L. Windus, *Computer Physics Communications*, 2010, 181, 1477-1489.
22. J. Wang, R. M. Wolf, J. W. Caldwell, P. A. Kollman and D. A. Case, *Journal of computational chemistry*, 2004, 25, 1157-1174.
23. V. Hornak, R. Abel, A. Okur, B. Strockbine, A. Roitberg and C. Simmerling, *Proteins*, 2006, 65, 712-725.
24. D. Case, T. Darden, T. Cheatham III, C. Simmerling, J. Wang, R. Duke, R. Luo, R. Walker, W. Zhang and K. Merz, *University of California, San Francisco*, 2010.
25. W. L. Jorgensen, J. Chandrasekhar, J. D. Madura, R. W. Impey and M. L. Klein, *The Journal of chemical physics*, 1983, 79, 926-935.
26. A. W. Gotz, M. J. Williamson, D. Xu, D. Poole, S. Le Grand and R. C. Walker, *Journal of chemical theory and computation*, 2012, 8, 1542-1555.
27. T. Darden, D. York and L. Pedersen, *The Journal of chemical physics*, 1993, 98, 10089-10092.
28. J.-P. Ryckaert, G. Ciccotti and H. J. Berendsen, *Journal of Computational Physics*, 1977, 23, 327-341.
29. S. Z. Grinter and X. Zou, *Molecules*, 2014, 19, 10150-10176.
30. N. Bharatham, K. Bharatham, A. A. Shelat and D. Bashford, *Journal of chemical information and modeling*, 2014, 54, 648-659.
31. M. R. Peluso, C. L. Miranda, D. J. Hobbs, R. R. Proteau and J. F. Stevens, *Planta medica*, 2010, 76, 1536-1543.
32. M. D. Vitorovic-Todorovic, C. Koukoulitsa, I. O. Juranic, L. M. Mandic and B. J. Drakulic, *European journal of medicinal chemistry*, 2014, 81, 158-175.
33. S. Shao, R. Yu, Y. Yu and Y. Li, *Journal of molecular modeling*, 2014, 20, 2399.
34. T. Paramo, T. J. Piggot, C. E. Bryant and P. J. Bond, *The Journal of biological chemistry*, 2013, 288, 36215-36225.
35. S. Sarkhel and G. R. Desiraju, *Proteins*, 2004, 54, 247-259.

Fig. 1

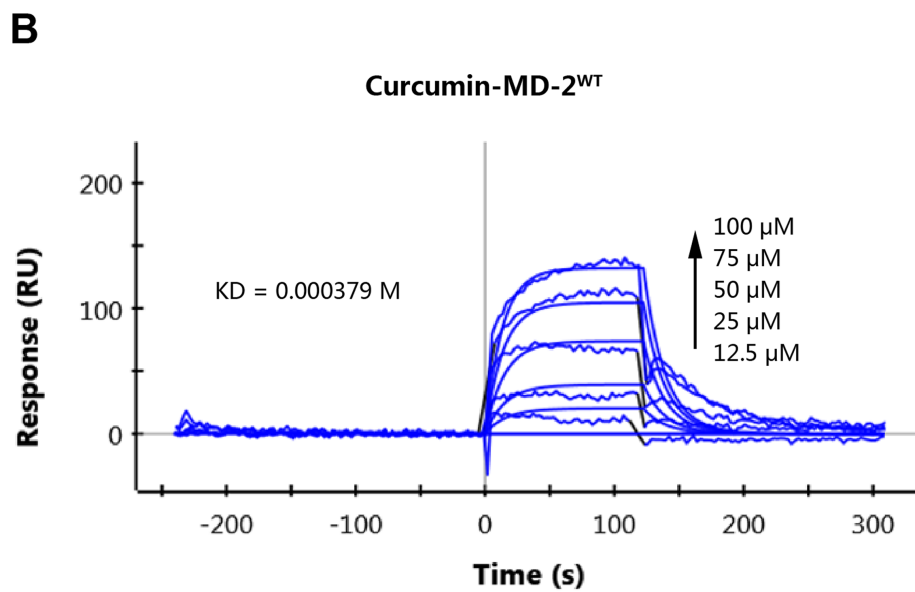
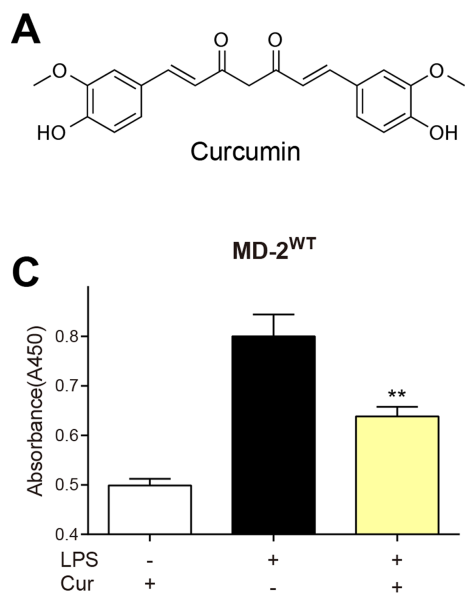


Fig. 2

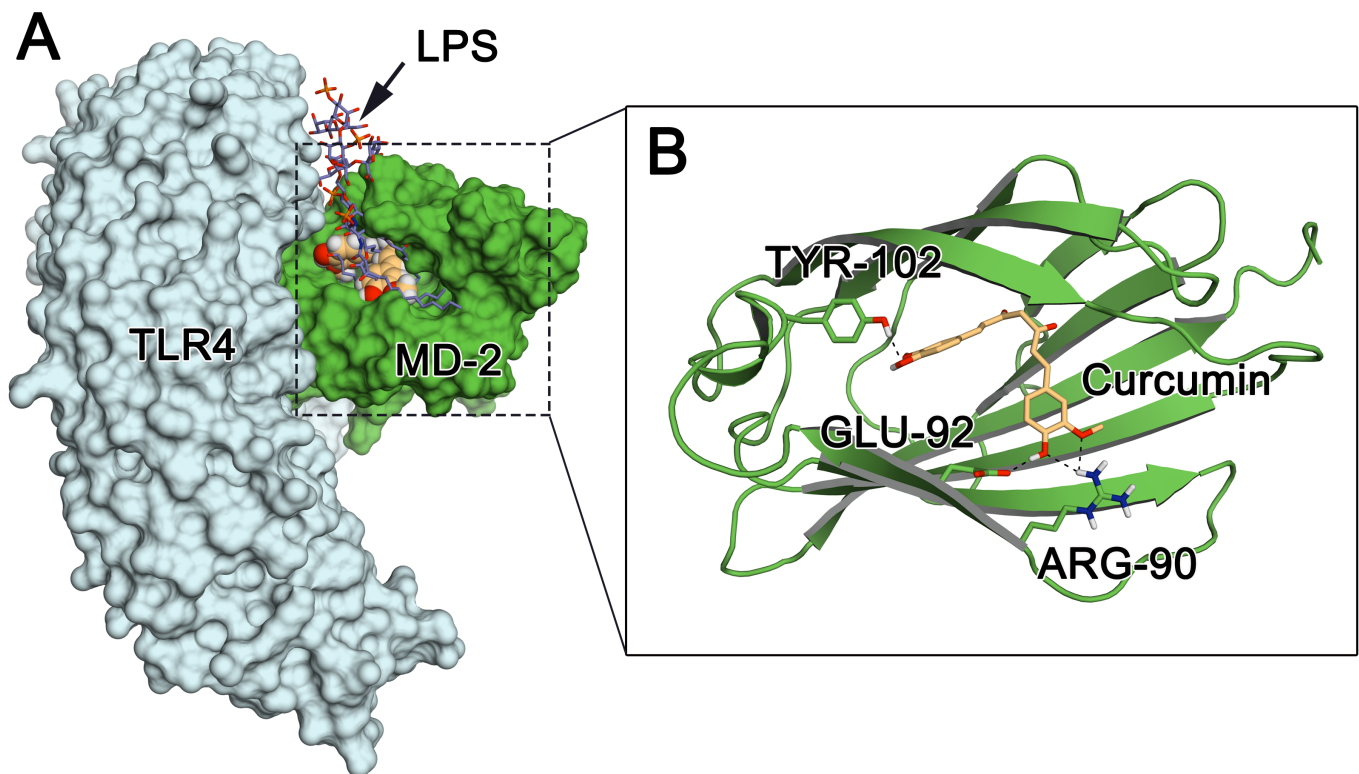


Fig. 3

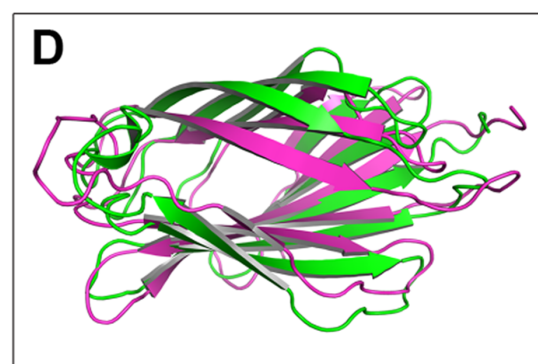
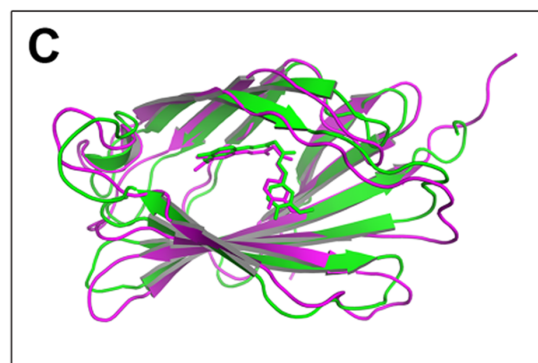
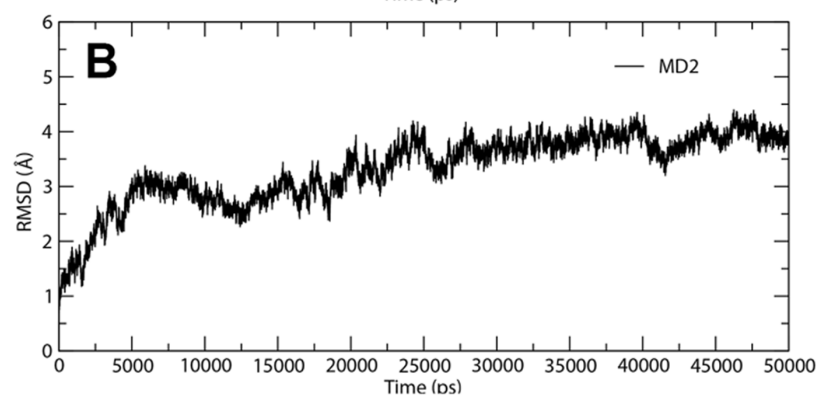
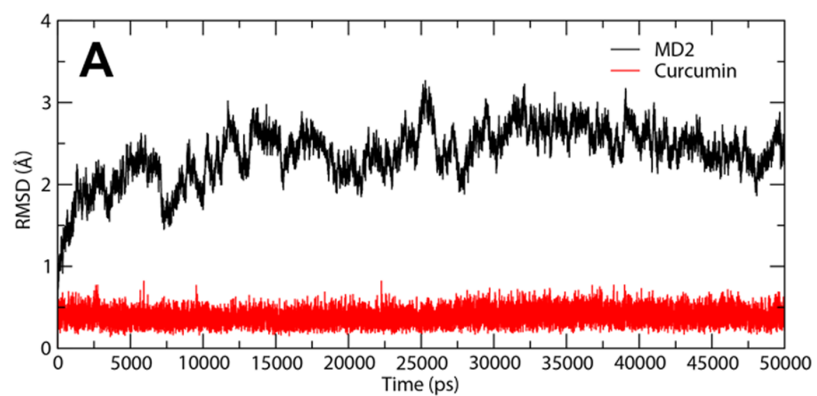


Fig. 4

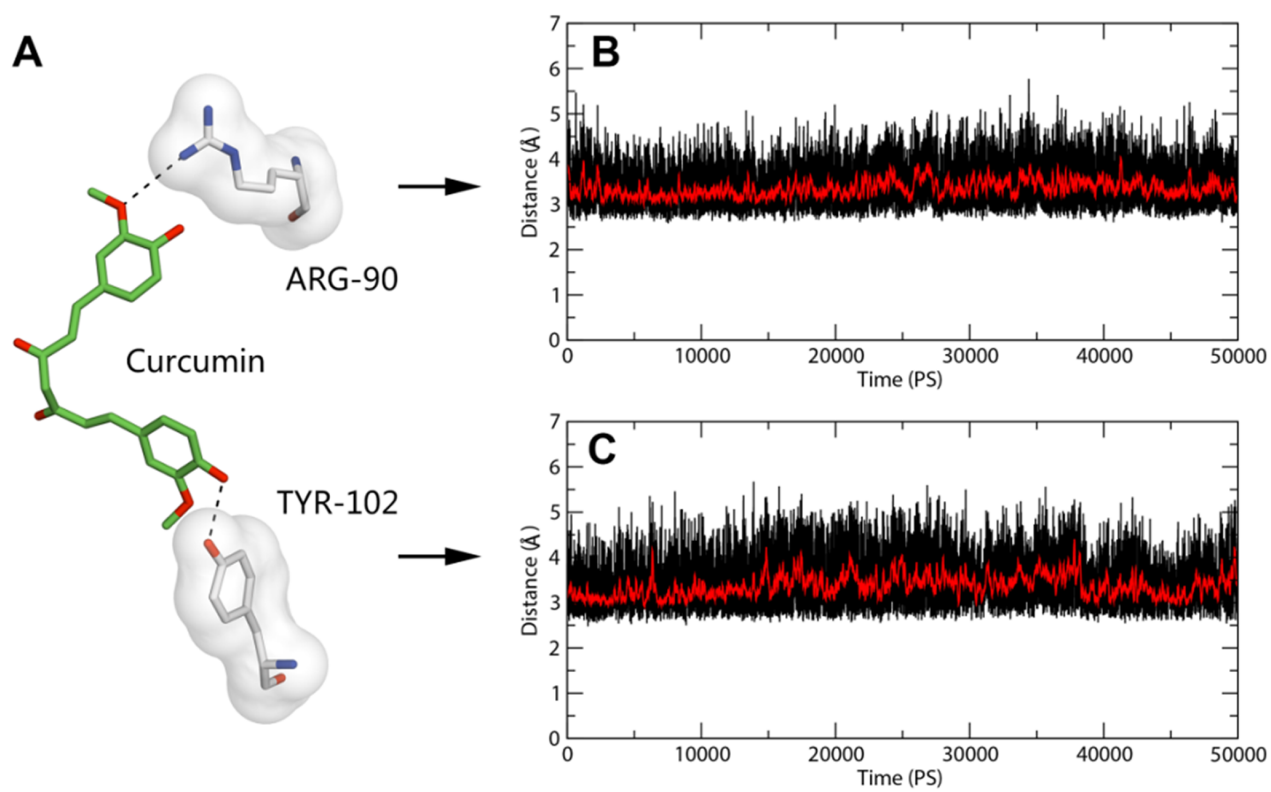


Table 1

System	Donor	Acceptor	Occupied (%)	Distance (Å)
Curcumin-MD2	ARG-90@NH1	Curcumin@O3	85.82	3.24 ± 0.26
	TYR-102@OH	Curcumin@O5	79.84	3.17 ± 0.30

Fig. 5

